Comparison of theoretical and simulation-based predictions of grain-boundary Kapitza conductance in silicon

Sylvie Aubry
Mechanics and Computation Group, Department of Mechanical Engineering, 496 Lomita Mall, Stanford University, Stanford, California 94305-4040, USA

Christopher J. Kimmer
Department of Physics and Astronomy, University of Louisville, Louisville, Kentucky 40292, USA

Ashton Skye
Advanced Material Processing and Analysis Center and Department of Physics, University of Central Florida, 4000 Central Florida Boulevard, Orlando, Florida 32816, USA

Patrick K. Schelling
Advanced Material Processing and Analysis Center and Department of Physics, University of Central Florida, 4000 Central Florida Boulevard, Orlando, Florida 32816, USA

(Received 12 February 2008; revised manuscript received 2 June 2008; published 18 August 2008)

We present a comparison between molecular-dynamics (MD) simulation and theoretical calculations using input from wave-packet simulations of the Kapitza conductance of two different grain boundaries in silicon. We find that for a $\Sigma 3(111)$ twin boundary with minimal disruption of the lattice, the Kapitza conductance is extremely high in contrast to previous results obtained for the $\Sigma 29(001)$ grain boundary. Theoretical predictions based on input from wave-packet simulations appear to show reasonable agreement with MD results for the $\Sigma 29(001)$ grain boundary but disagreement by a factor of about ten for the $\Sigma 3(111)$ boundary. The origin of the apparent discrepancies is analogous to previously noted difficulties in comparing theoretical predictions to experimental measurements of the Kapitza conductance. We show why the apparent discrepancies are large when the interface phonon transmission is high and relatively small when the phonon transmission is low. We demonstrate how the theoretical predictions and MD simulation results can be compared in a consistent and meaningful way, thereby removing the apparent contradictions. These questions also are discussed in the important context of relating MD results to experimental observations.

DOI: 10.1103/PhysRevB.78.064112 PACS number(s): 07.05.Tp

I. INTRODUCTION

As devices become smaller and smaller, material geometries such as grain boundaries increasingly dominate heat transfer processes. Understanding how grain boundaries and, more generally, material geometries affect thermal transport in semiconductors is thus nowadays indispensable.

At grain boundaries or interfaces between dissimilar materials, there is an added resistance to phonon-mediated heat transport.[1,2] The thermal resistance, usually called the Kapitza resistance, results in a temperature discontinuity ΔT at the interface. The Kapitza resistance R_K relates the thermal current J to the observed temperature discontinuity ΔT as $J=\frac{\Delta T}{R_K}$. Alternately, it is often convenient to consider the Kapitza conductance $\sigma_K=\frac{1}{R_K}$ especially when details of the transport properties at the interface are considered.

Theoretical studies usually rely on the acoustic-mismatch (AM) or diffuse-mismatch (DM) models, which make predictions for σ_K using simple descriptions of interfacial phonon scattering. Molecular-dynamics (MD) simulation has recently emerged as a promising approach for investigating phonon scattering.[3–5] While MD can determine σ_K within a single simulation, it is still important to relate the fundamental phonon-scattering properties to the overall σ_K. By establishing a direct relationship between phonon scattering and σ_K, important insight can be obtained to establish the relevance of simple theoretical models. In addition, by gaining further insight into the details of scattering at the interface, it might be possible to engineer interfaces that have tailored properties such as very high or low σ_K.

With the goal of obtaining detailed insight into interfacial scattering properties, the wave-packet simulation method was developed.[4–6] The basic idea is to create localized wave packets through a superposition of normal modes of a bulk perfect crystal. The wave packets are then propagated using MD simulation. After interacting with an interface, the energy-transmission coefficient $\alpha(\lambda,\vec{k})$ is determined for each polarization λ and wave vector $\vec{k}$ as the fraction of incident energy that propagates across the interface. To determine σ_K, we use the expression[7,8]

$$\sigma_K(T)=\frac{1}{\Omega}\sum_{\lambda,\vec{k}}^{+}\hbar\omega(\lambda,\vec{k})v_z(\lambda,\vec{k})\frac{\partial N_0[\omega(\lambda,\vec{k}),T]}{\partial T}\alpha(\lambda,\vec{k}), \quad (1)$$

where Ω is the system volume, $\omega(\lambda,\vec{k})$ is the frequency of a normal mode with polarization λ and wave vector $\vec{k}$, $v_z(\lambda,\vec{k})$ is the component of the phonon group velocity perpendicular to the interface plane, and $N_0[\omega(\lambda,\vec{k}),T]$ is the equilibrium Bose distribution. The plus sign on the summation indicates

that modes with positive group velocity only are included. It is important to note that this expression is applicable for grain boundaries where the material on either side of the interface is identical. For heterointerfaces, the modes on either side of the interface have to be explicitly included in an expression for σ_K. To compare Eq. (1) with direct MD simulation, it is necessary to take the high-temperature or classical limit since MD is a classical simulation method. We have previously shown[6] that the predictions using Eq. (1) with $\alpha_{\lambda\vec{k}}$, determined using wave-packet simulations, agree fairly well with direct MD simulation for the case of a high-energy $\Sigma 29(001)$ grain boundary in silicon. In particular, using Eq. (1) we obtained $\sigma_K=0.68$ GW/m^2 K, compared with $\sigma_K=0.80$ GW/m^2 K, as determined with direct MD simulation at $T=500$ K.

In this paper, we present results for a $\Sigma 3(111)$ twin boundary in silicon that show dramatic disagreement between the predictions of Eq. (1) and the results of direct MD simulation. We show that this situation is analogous to the conceptual difficulties encountered in relating theoretical models to experiment. In particular, it has been shown by Katerberg *et al.*,[9] and also Pettersson and Mahan[8] that comparison between experiment and theory depends on an understanding of what temperature difference ΔT is measured in an experiment. We propose a simple modification to Eq. (1) that improves dramatically the agreement between theoretical predictions and direct MD simulation for the case of weak phonon scattering at the highly ordered $\Sigma 3(111)$ grain boundary. For the case of strong scattering at the disordered $\Sigma 29(001)$ grain boundary, where the agreement between Eq. (1) and MD simulation is already reasonably good, the modification of Eq. (1) has a much smaller effect.

In the next section, we describe the simulation details. In Sec. III, we present the results including a comparison between predictions using Eq. (1) and direct MD results. We also develop a modification of Eq. (1), and demonstrate improved agreement between the theoretical predictions and the MD simulations. In the last section, we present the discussion and conclusions, including some insights into how bulk and interface properties might be coupled.

II. METHODOLOGY

We obtained the structure used to study the $\Sigma 3(111)$ grain boundary by first orienting the crystal so that the [111] direction lies along the z axis of the simulation cell. We then define a (111) plane at $z=0$ and rotate atoms above this plane by $\phi=60°$ about a [111] axis while keeping the atoms below the plane fixed. This operation does not change any of the bond lengths or angles at the interface but does disrupt the periodicity of the perfect-crystal lattice. A cross section of the resulting interface is shown in Fig. 1. Periodic boundary conditions were applied in all three dimensions resulting in two grain boundaries in the supercell. The dimensions of the supercell in the grain-boundary plane (i.e., the $x-y$ plane) were $L_x=3\sqrt{\frac{3}{2}}a$ and $L_y=5\sqrt{\frac{1}{2}}a$. The length of the simulation cell along the z axis was chosen to be $L_z=600\sqrt{3}a$. The entire simulation cell had 108 000 atoms. We made two different calculations of transmission coefficients and Kapitza conductance for two different system sizes. All the results presented below are for the larger system described above unless mentioned otherwise.

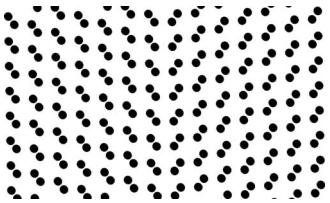

FIG. 1. A cross section of the $\Sigma 3(111)$ grain boundary.

We used the Stillinger-Weber (SW) potential for silicon that results in a lattice parameter $a=0.543$ nm.[10] Because the bond lengths and bond angles in this structure are unchanged from the bulk perfect crystal, the SW potential predicts no energy difference between bulk and grain-boundary atoms. Consequently, the $\Sigma 3(111)$ grain boundary is a zero-energy grain boundary with the SW potential. This is due to the short-ranged nature of the SW potential and is despite the physical fact that any disruption of the lattice periodicity should result in some increase in the potential energy. Nonetheless, the energy of this twin boundary is expected to be very low even with a more realistic interatomic potential. Furthermore, the loss of periodicity at the interface will still result in phonon scattering. We therefore believe that this model is appropriate for the problem at hand although undoubtedly the quantitative results may be different for a more realistic potential.

We perform MD simulations to determine the Kapitza conductance using both the direct method and the wave-packet method. More details about the direct heat flux method can be found in Refs. 3–5, and more details about the lattice dynamics method can be found in Ref. 6 and references therein. In the direct method, a heat source and sink are used to generate a thermal current within a MD simulation. The thickness of the heat source and sink was $10a$ (i.e., 5.43 nm). At every MD time step, 9×10^{-4} eV of kinetic energy was added to the source region and removed from sink region by rescaling the velocities of the atoms. Given the dimensions of the simulation supercell described above and the MD time step of $dt=0.55$ fs, the heat current was about $J=33.9$ GW/m^2. While this is rather large compared to some previous studies, we have found that a large heat current is necessary to establish a significant temperature discontinuity at the interface. The simulation began with 0.05 ns of simulation time at a constant temperature of $T=500$ °K, followed by 4.77 ns of simulation with the heat source and sink turned on. To obtain time-averaged temperature profile, we included only the last 4.20 ns of the simulation. We have verified that the temperature profile is very steady for the final 4.20 ns of the simulation, demonstrating that the system readily achieves a steady state. We made a linear fit to the temperature gradient on either side of the interfaces and use the difference in the temperature at the interface, determined from the fits, to compute ΔT.

For wave-packet simulations, we used the same approach described in an earlier work.[6] We determined the energy-transmission coefficients $\alpha(\lambda,\vec{k})$ as a function of wave vec-

tors $\vec{k}$ and acoustic branch λ using MD. The first Brillouin zone was sampled by performing a simulation for each branch λ. The wave vector components k_x and k_y are fixed for each simulation while k_z (i.e., the component normal to the interface) is varied for each wave packet. We considered 41 wave vectors in this study. The central wave vector and frequencies of each wave packet is chosen to achieve a uniform-frequency sampling of the dispersion relation for each branch. One simulation for each branch and pair (k_x, k_y) consistent with the periodic simulation box was performed. Typically, simulations for optical modes are prohibitively expensive because group velocities are rather low, requiring long simulation times. As described below, we estimate the contribution from the optical branches based on a few limited simulations of longitudinal optical (LO) modes with normal incidence on the boundary.

We have performed simulations corresponding to a complete set of non-normal-incidence phonon branches for LA and TA modes. Each branch was sampled at a frequency interval of 0.8 THz. In other words, a separate wave packet was added to the simulation for each 0.8 THz of frequency. As previously noted,[6] the accuracy of the quadrature used to evaluate Eq. (1) can be investigated. We find that the 0.8 THz sampling is accurate to within 15% in the high-temperature limit.

III. SIMULATION RESULTS AND THEORY PREDICTIONS

In Fig. 2 we show the computed temperature profile in the MD simulation cell using the direct method. The temperature discontinuity is extremely small, indicating that the grain boundary is having a very small effect on the thermal transport.

To compute the temperature discontinuity, we made a linear fit to data within 10 nm of the grain boundaries excluding a region of 1 nm on either side. The discontinuity was determined from the difference in temperature between the two fits determined right at the grain-boundary interface. The temperature discontinuities are 3.49 and 3.13 K at the two boundaries. The average for the two grain boundaries gives $\Delta T = 3.31$ K. Using this value and the incident heat current $J = 33.9$ GW/m^2, we obtain $\sigma_K = 10.2$ GW/m^2 K. We estimate the uncertainty in ΔT as ± 0.5 K. The uncertainty in ΔT leads to some potential error in the computed value of σ_K. The temperature gradient fits on either side of the grain-boundary interface appear noticeably different in Fig. 2(b). The differences appear to be within the statistical error inherent in the temperature profiles. In this case, because the fits are made only near the boundary in order to get the best estimate of ΔT, the linear fits are made into smaller sample of data and as a result contain more statistical errors. However, we can definitively place σ_K between 9.0 and 12.0 GW/m^2 K. This is the largest computed value of σ_K for an Si grain boundary by nearly a factor of about ten and is comparable to some values recently obtained for diamond grain boundaries.[11]

The wave-packet simulations confirm the expectation that interfacial scattering is very weak. In Fig. 3 we show the transmission coefficient versus frequency for several LA

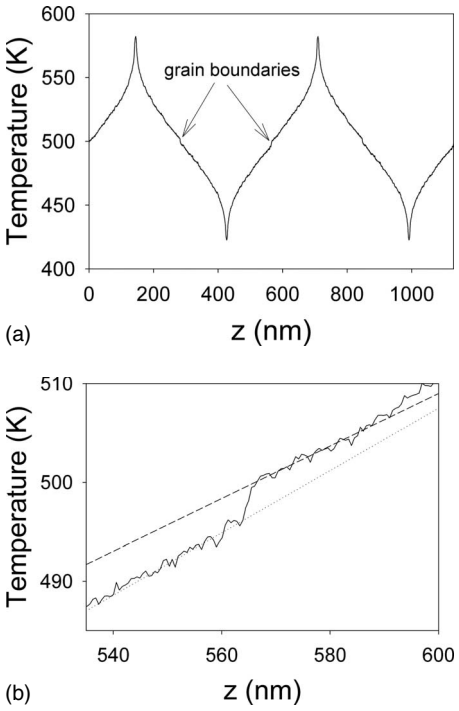

FIG. 2. Time-averaged temperature profile obtained from direct MD simulation of thermal transport through Σ3 grain boundaries. (a) The boundary positions are at about $z=282$ and 565 nm. The actual simulation cell spans from $z=0$ to 565 nm. (b) The temperature near the grain boundary at $z=565$ nm is shown in closer perspective to see the temperature discontinuity at $z=565$ nm. The dotted and dashed lines are linear fits made near the boundary used to compute the temperature discontinuity at the grain boundary

branches. With the exception of some of the high-frequency modes, the scattering of LA modes is almost imperceptible with $\alpha \sim 1$ for much of the spectrum. By contrast, TA modes display somewhat stronger scattering, as shown in Fig. 4. Results presented in Figs. 3 and 4 are for a system $L_z = 600\sqrt{3}a$ long. We have calculated transmission coefficients for a smaller system for comparison. Both systems give very similar results. In comparison to previous results for the Σ29(001) grain boundary,[6] strong correlation between frequency and α is less apparent. For example, while the LA modes seem to scatter only for frequencies above ~10 THz,

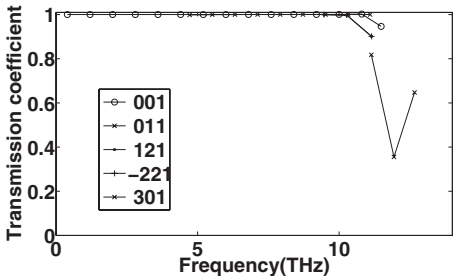

FIG. 3. Energy-transmission coefficients as a function of frequency computed for various LA branches. Each branch is labeled by the particular values of m and n as [mn1]. For instance, the case of normal incidence corresponds to the branch labeled [001] (i.e., $m=0$ and $n=0$).

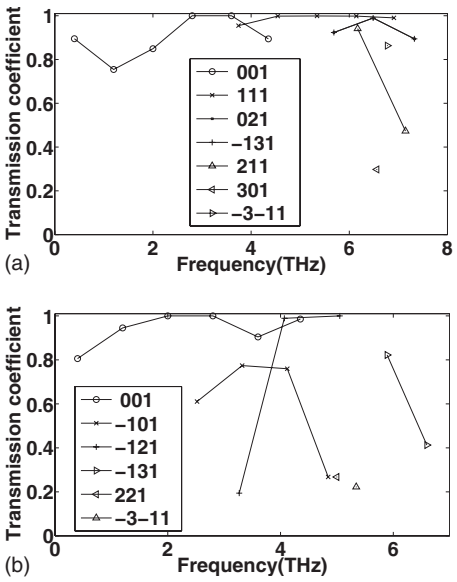

FIG. 4. (a) Transmission coefficient plotted as a function of frequency for various TA branches polarized along $[10\bar{1}]$. (b) Transmission coefficient plotted as a function of frequency for various TA branches polarized along $[\bar{1}2\bar{1}]$.

the TA modes show much stronger dependence on the particular wave vector and polarization. In general, the computed values of α for the current study are much higher in comparison to those found for the $\Sigma 29(001)$ grain boundary.

Figure 5 shows the results for the calculation of the Kapitza conductance using Eq. (1). We use wave-packet simulations only to determine α for the LA and TA modes. To estimate the contribution from the optical branches, we assume $\alpha=0.25$ for all of the optical branches. This value is based on our previous study of a few optical modes incident on the $\Sigma 29(001)$ grain boundary. The results are shown for the acoustic modes both with and without the estimated contribution from the optical modes. We see from Fig. 5 that the LO and TO modes account for about 10% of the energy transport. For comparison, we have also added to Fig. 5 the prediction based on the DM model, which, for a grain boundary, corresponds to $\alpha=0.5$. Not surprisingly, the relatively large values of α obtained from the wave-packet simulations yield predictions for σ_K that are significantly higher than the DM model. To explore finite-size effects, we also studied a smaller system with $L_x=2\sqrt{\frac{3}{2}}a$, $L_y=2\sqrt{\frac{1}{2}}a$, and $L_z=300\sqrt{3}a$ with a total of 24 000 atoms. We find for this smaller system a value of σ_K that is only about 8% higher than the results found for the larger system. This indicates that the larger simulated system represents an adequate sampling of the Brillouin zone. Finally, we also determined σ_K in the so-called radiation limit where $\alpha=1$ for the entire spectrum. In the high-temperature limit where classical statistics are valid, we obtain $\sigma_K=1.96$ GW/m^2 K.

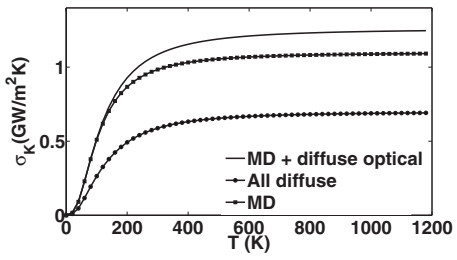

FIG. 5. The Kapitza conductance σ_K computed using Eq. (1) with transmission coefficients determined from MD simulation (dashed line). The solid line shows the calculated Kapitza conductance using the MD data for the acoustic branches plus an assumed uniform transmission coefficient of 0.25 for the optical branches. The lowest curve shows σ_K assuming diffuse scattering for the acoustic branches and a transmission coefficient of 0.25 for the optical modes.

TABLE I. Values of σ_K in GW/m^2 K determined by direct MD simulation and theoretical calculations based on Eqs. (9) and (10) with input from wave-packet simulations. Results for direct MD simulation and theory based on Eq. (1) of the $\Sigma 29(001)$ grain boundary are taken from Ref. 6. The theoretical predictions given include estimated contributions from the optical branches.

Method	$\Sigma 3(111)$	$\Sigma 29(001)$
Direct MD ($T=500$ K)	10.2	0.80
Theor. [Eq. (1)]	1.23	0.68
Theor. [Eq. (9)]	8.35	1.52
Theor. [Eq. (10)]	6.34	1.40

Comparison between the theoretical predictions and the direct MD simulation results apparently exhibit a very large discrepancy for the $\Sigma 3(111)$ grain boundary. The relevant comparisons between the direct MD result and theoretical calculations based on Eq. (1) are shown in Table I. The theoretical predictions that use the wave-packet result give a value of nearly 63% in the radiation limit. This demonstrates the very weak scattering of the interface and also can somewhat justify the assumption of $\alpha=0.25$ for the optical modes. In particular, even when we assume optical modes are strongly scattered, we obtain a value for σ_K that is not much less than the radiation limit. By contrast, the direct MD simulation results in a value for σ_K that is *much greater* than the radiation limit.

The rather dramatic disagreement between the theoretical model and the direct MD simulations has a straightforward explanation. The origin of the disagreement has been discussed by previous authors in the slightly different but closely related context of comparing theoretical predictions based on the AM, DM, or a more general model represented by Eq. (1), to experiment. In particular, it has been noted that in the limit of $\alpha=1$ (i.e., the radiation limit), the theory predicts a finite resistance. This seems contradictory especially when one considers that $\alpha=1$ is what one expects for an imagined interface in an ideal crystal.

However, Pettersson and Mahan[8] have previously shown that the origin of the difficulty is in understanding exactly what temperature difference ΔT is measured in experiment. For example, they observed that for an imagined interface with $\alpha=1$, if the temperature difference ΔT is determined from the phonon distribution *incident* on the interface, Eq. (1) can be shown to be consistent with the usual theory of thermal diffusion. This observation suggests that Eq. (1) is

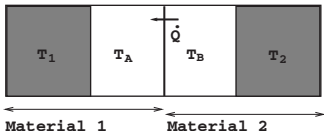

FIG. 6. The different temperatures involved in the direct heat flux method ($\Delta T = T_b - T_a$) and the lattice dynamics method ($\Delta T = T_2 - T_1$).

appropriate in spite of the apparent paradox that R_K is finite even for an imagined interface.

Within the context of the AM model, the analogous theory to that presented in Eq. (1) due to Little[12] leads to a prediction $\sigma_K = 4\epsilon_1 \alpha_{12} T^3$, where ϵ_1 is a parameter for material 1 and α_{12} is the energy-transmission coefficient for phonons incident from materials 1 to 2, averaged over all possible angles of incidence. It was noted by Simons[13] that, in addition to giving a finite resistance for an imagined interface, the phonon distribution used in the Little model did not result in a thermal current in the bulk. Using a nonequilibrium phonon distribution within the AM model, Simons[13] obtained the expression $\sigma_K = (4\epsilon_1 \alpha_{12} T^3)(1 - \frac{1}{2}\beta_{12} - \frac{1}{2}\beta_{21})^{-1}$, where β_{12} and β_{21} are parameters closely related to α_{12}. When the interface weakly scatters phonons and the limit $\alpha \to 1$ applies, it is appropriate to take $\alpha_{12} = \beta_{12} = \beta_{21}$. In the Simons theory, when an interface has $\alpha = 1$ (i.e., an imagined interface), then σ_K is infinite and $R_K = 0$. Comparison of the Little and Simons theories shows that they make similar predictions for σ_K when scattering is very strong (i.e., small α) but exhibit strong disagreement when scattering is weak (i.e., $\alpha \sim 1$).

While the Little and Simons theories at first sight appear to be incompatible, Katerberg *et al.*[9] showed that they are in fact equivalent as long as one knows exactly how to define ΔT. The relevant temperatures are shown schematically in Fig. 6. Katerberg *et al.*showed that the Little theory is appropriate if the temperatures used to determine ΔT are consistent with the distribution of phonons *incident* on the interface. In other words, if a thermometer is in fact measuring the distribution of incident phonons with temperatures T_2 and T_1, then the Little theory is appropriate. By contrast, if the thermometer in the experiment is measuring the phonon distribution *near* the interface (i.e., $\Delta T = T_b - T_a$ in Fig. 6), then the Simons theory is appropriate.

In light of these considerations, the apparently strong disagreement between direct MD results and the wave-packet predictions used in Eq. (1) can be understood. In the direct MD simulation, the temperature difference we use to compute ΔT is equivalent to $T_b - T_a$ in Fig. 6. However, based on the observations by Katerberg *et al.*, the theory given by Eq. (1) should be appropriate when the temperature difference is characteristic of the phonon distribution *incident* on the interface (i.e., $\Delta T = T_2 - T_1$ in Fig. 6). In the case of the $\Sigma 3(111)$ grain boundary, the wave-packet results indicate that much of the spectrum corresponds to the limit $\alpha \to 1$. In this limit, we expect the disagreement between the theoretical prediction from Eq. (1) and direct MD results to be large. As we have shown in Table I, it is indeed the case.

To bring the theoretical predictions into better agreement with direct MD results, it is necessary to make the appropriate comparison. Two possible approaches exist. One approach is to attempt to compute or estimate the temperature distribution of the normal modes *incident* on the interface. The other approach is to attempt to modify the theory in a manner analogous to the Simons AM model predictions.

Directly computing the distribution of normal modes incident on the interface is not a simple task. In principle, the atomic displacements and velocities can be used to compute the distribution of normal modes near the interface, and isolate those that are incident on the interface from those that are traveling away from the interface. This is certainly possible but would be extremely computationally intensive because the distribution of energy in each normal mode would have to be time averaged over the entire MD simulation. Also, the displacements and velocities would have to be convoluted with a window function (e.g., a Gaussian window) near the interface to isolate the relevant distributions. Alternately, a simple estimate can be made that illustrates the appropriate comparison. It has previously been shown[3] that the mean-free path in SW silicon is about $l_\infty = 100$ nm for $T = 500$ K. We follow Pettersson and Mahan,[8] and assume that the temperature of normal modes incident on the interface can be determined from the local average temperature one mean-free path away from the interface. In particular, using T_2 and T_1 to refer to the temperatures associated with modes incident on the interface at angle of incidence θ, we find

$$T_1 = T - \frac{T_b - T_a}{2} - \frac{dT}{dz} l_\infty \cos\theta, \tag{2}$$

and

$$T_2 = T + \frac{T_b - T_a}{2} + \frac{dT}{dz} l_\infty \cos\theta. \tag{3}$$

For the simulation of the $\Sigma 3(111)$ boundary, we find that there is substantial nonlinearity in the temperature profile within about 10 nm of the grain-boundary interface. In particular, linear fits to the profile shown in Fig. 2 within 10 nm of grain boundaries results in an average gradient of about 0.264 K/nm. By contrast, if we neglect the region within 10 nm of the grain boundaries, and also the region within 70 nm of the heat source and sink, we compute an average gradient of 0.337 K/nm. These slightly smaller temperature gradients near the grain-boundary interface might indicate the presence of partially ballistic transport. Because the mean-free path is ~ 100 nm, we assume here that the gradient far from the interface is more appropriate for an estimate of T_1 and T_2. Averaging over angles and including the $T_b - T_a = 3.31$ K discontinuity at the grain boundary, we obtain $\Delta T = T_2 - T_1$ to be about 37.01 K. Using this value for ΔT instead of the 3.31 K used to obtain σ_K in Table I, we find $\sigma_K = 0.92$ GW/m^2 K. Even with this very rough estimate, the comparison to the theoretical prediction of $\sigma_K = 1.23$ GW/m^2 K is already quite reasonable.

For the $\Sigma 29(001)$ grain boundary, wave-packet simulations and direct MD already are in reasonable agreement. In this case, the corrections are relatively small because the computed temperature discontinuity at the interface is large.

The approximate temperature gradient for the $\Sigma 29(001)$ grain-boundary simulations was 0.27 K/nm with an applied thermal current of $J=15.36$ GW/m^2. The temperature discontinuity at the grain boundary from a previous MD study[5] was found to be 19.2 K. Applying the same estimates as above to obtain the temperature of the normal modes incident on the grain boundary, we obtain for $\Delta T=T_2-T_1$ a value of about 46.2 K. Using this temperature difference, we obtain the estimate $\sigma_K=0.33$ GW/m^2 K. This is smaller by just over a factor of two from σ_K estimated from the discontinuity of 19.2 K, determined from $\Delta T=T_b-T_a$ (i.e., from the temperatures near the grain boundary).

The main point to make is that estimated corrections permitting meaningful comparisons between the theoretical calculations and direct MD simulation are relatively small for the strongly scattering $\Sigma 29(001)$ grain boundary. By contrast, the estimated corrections are large for the case of weak scattering at the $\Sigma 3(111)$ grain boundary. This is consistent with Katerberg *et al.*'s observation that the Little and Simons theories should disagree most strongly when the scattering is weak.[9]

Next, we consider an alternate theory to that in Eq. (1) that can be compared directly to the MD simulation where ΔT is determined in the usual way from the temperature discontinuity at the interface (i.e., $\Delta T=T_b-T_a$). From Katerberg *et al.*,[9] it is clear that we need something equivalent to the Simons theory but more generally applicable beyond the AM model for phonon scattering. We begin by expressing the current in terms of the temperature distribution of normal modes incident on the interface. For waves incident on the grain boundary at temperatures T_1 and T_2, we have

$$J=-\frac{1}{\Omega}\sum_{\lambda\vec{k}}^{+}\hbar\omega(\lambda,\vec{k})v_z(\lambda,\vec{k})\alpha(\lambda,\vec{k})\frac{dN_0[\omega(\lambda,\vec{k}),T]}{dT}(T_2-T_1). \tag{4}$$

The next step is to relate T_b-T_a to the temperature difference T_2-T_1. It is first important to note that the relevant temperature for each normal mode will depend on where the last scattering event in the bulk occurred. In other words, T_2-T_1 should be considered depending on the particular mode in branch λ with wave vector $\vec{k}$. We introduce $\tau(\lambda,\vec{k})$ as the phonon lifetime to give the temperature of the incident waves in analogy to Eqs. (2) and (3),

$$T_1=T-\frac{T_b-T_a}{2}-\frac{dT}{dz}v_z(\lambda,\vec{k})\tau(\lambda,\vec{k}), \tag{5}$$

and

$$T_2=T+\frac{T_b-T_a}{2}+\frac{dT}{dz}v_z(\lambda,\vec{k})\tau(\lambda,\vec{k}). \tag{6}$$

If we take the interfacial current given by Eq. (4) and set it equal to the standard expression for the bulk current in the presence of a temperature gradient $\frac{dT}{dz}$,

$$J=-\frac{1}{\Omega}\sum_{\lambda\vec{k}}\hbar\omega(\lambda,\vec{k})v_z^2(\lambda,\vec{k})\tau(\lambda,\vec{k})\frac{dN_0[\omega(\lambda,\vec{k}),T]}{dT}\frac{dT}{dz}, \tag{7}$$

and then use $J=\sigma_K(T_b-T_a)$ to define the σ_K (i.e., in terms of the discontinuity at the interface T_b-T_a), we obtain

$$\sigma_K=\frac{1}{\Omega}\left[\sum_{\lambda\vec{k}}^{+}\hbar\omega(\lambda,\vec{k})v_z(\lambda,\vec{k})\alpha(\lambda,\vec{k})\frac{dN_0}{dT}\right]\times\frac{\left[\sum_{\lambda\vec{k}}\hbar\omega(\lambda,\vec{k})v_z^2(\lambda,\vec{k})\tau(\lambda,\vec{k})\frac{dN_0}{dT}\right]}{\sum_{\lambda\vec{k}}\hbar\omega(\lambda,\vec{k})v_z^2(\lambda,\vec{k})\tau(\lambda,\vec{k})[1-\alpha(\lambda,\vec{k})]\frac{dN_0}{dT}}. \tag{8}$$

This expression is derived to apply to the case where the temperature discontinuity is defined in terms of the temperatures near the interface (i.e., $\Delta T=T_b-T_a$). When Eq. (8) is applied to the case of an imagined interface with $\alpha=1$ for each mode, we see that σ_K diverges. This means that for an imagined interface, $R_K=0$ and $T_b-T_a=0$. By contrast, the theoretical expression for σ_K in Eq. (1) is finite for the limit $\alpha=1$. While Eqs. (1) and (8) make very different predictions when $\alpha\to 1$, in the limit where $\alpha\to 0$, the two expressions converge to the same result. It is clear that Eq. (8) is comparable to the Simons theory whereas Eq. (1) is closely related to approach due to Little. Hence, we expect that Eq. (8) is appropriate for comparison to MD simulation results when σ_K is defined in terms of the temperature discontinuity T_b-T_a.

To compare the predictions made by Eq. (8) directing MD simulation, we have to evaluate the summations in some approximation because $\tau(\lambda,\vec{k})$ is not exactly known. One reasonable approximation is to assume a constant relaxation time τ for each normal mode due to anharmonic phonon-phonon interactions. We also take the limit of classical statistics where the heat capacity of each mode is k_B. In this approximation, the expression for the Kapitza conductance is

$$\sigma_K=\frac{\frac{k_B}{\Omega}\left[\sum_{\lambda\vec{k}}^{+}v_z(\lambda,\vec{k})\alpha(\lambda,\vec{k})\right]\left[\sum_{\lambda\vec{k}}v_z^2(\lambda,\vec{k})\right]}{\sum_{\lambda\vec{k}}v_z^2(\lambda,\vec{k})[1-\alpha(\lambda,\vec{k})]}. \tag{9}$$

Another reasonable approach is to assume a constant mean-free path. In other words, if we assume that for each mode $v_z(\lambda,\vec{k})\tau(\lambda,\vec{k})$ is a constant independent of λ and $\vec{k}$, we then obtain the expression

$$\sigma_K=\frac{\frac{k_B}{\Omega}\left[\sum_{\lambda\vec{k}}^{+}v_z(\lambda,\vec{k})\alpha(\lambda,\vec{k})\right]\left[\sum_{\lambda\vec{k}}^{+}v_z(\lambda,\vec{k})\right]}{\sum_{\lambda\vec{k}}^{+}v_z(\lambda,\vec{k})[1-\alpha(\lambda,\vec{k})]}. \tag{10}$$

A comparison of the predictions using Eqs. (1), (9), and (10) is given in Table I. We see from the results in Table I that Eq. (9) appears to agree more closely with direct MD. In

particular, the results for the $\Sigma 3(111)$ grain boundary are in much better agreement whereas the $\Sigma 29(001)$ results remain reasonably close. It is important to acknowledge that while the $\Sigma 3(111)$ results are in much better agreement with either Eq. (9) or Eq. (10), the $\Sigma 29(001)$ grain boundary is actually in slightly better agreement with Eq. (1). However, we believe that the approach outlined here is more appropriate than the previous approach based on Eq. (1).

The transmission coefficient within a particular phonon branch for the $\Sigma 29(001)$ grain boundary has been observed to be primarily a function of the incident phonon frequency $\omega(\lambda,\vec{k})$.[6] To estimate the uncertainty in any estimates using the available MD data, and Eqs. (9) and (10), we fit the $\Sigma 29(001)$ data to a quintic polynomial function of frequency for each phonon branch. With the fit function, the convergence of the summations over the first Brillouin zone can be studied for various sampling or discretization schemes. We determine the relative difference between the uniform-frequency sampling scheme used to sample the Brillouin zone with MD and the complete summation over wave vectors compatible with the periodic simulation cell. We obtain an error of 24.5% for Eq. (9) and an error of 9.25% for Eq. (10). The uncertainty using Eq. (1) is 16%, which shows that assuming the $v_z\tau$ to be constant tends to reduce the uncertainty while assuming the relaxation-time constant tends to increase it. These trends in the uncertainties can follow from the general observation that the modes with smallest $\vec{k}$ tend to have $\alpha \rightarrow 1$ while those with the smallest group velocity tend to $\alpha \rightarrow 0$. The smallest-$\vec{k}$ modes with high transmission (i.e., those having large group velocity) are weighted the most, leading to greater relative error due to the v_z^2 term in Eq. (10).

We cannot make the same comparison for the $\Sigma 3(111)$ grain boundary because the transmission coefficients are not as well approximated as a function of frequency. We can, however, examine the convergence of the sum in each formula that is independent of the transmission coefficient. We estimate an error of 14% in the calculations of the sum in the numerator of Eq. (9) and an error of 5% for Eq. (10). For the $\Sigma 29(001)$ grain boundary, the uncertainties in these formulas follow the same trends noted in the previous paragraph with an uncertainty of 18.3% from Eq. (9) and 6.8% for Eq. (10).

We discuss some of the limitations and uncertainties that remain in the next section.

IV. DISCUSSION AND CONCLUSIONS

We have presented results for phonon scattering and Kapitza conductance for two different grain boundaries in silicon. In comparing theoretical predictions to MD simulation results, we have shown that it is important to consider the appropriate definition for the temperature discontinuity. When MD simulation uses the temperature discontinuity at the interface $T_b - T_a$ shown in Fig. 6, then it is more appropriate to use a definition for σ_K given by either Eq. (9) or Eq. (10) than Eq. (1). In the case of weak interfacial scattering, such as the $\Sigma 3(111)$ grain boundary studied here, the modified expressions for σ_K in Eq. (9) or Eq. (10) are able to treat the limit where σ_K exceeds the so-called radiation limit.

As Katerberg had previously shown when contrasting the Simons and Little theories, the difficulty lies in understanding what approach is equivalent to experiment. In particular, it is important to understand whether the experimental system measures the discontinuity at an interface as $T_2 - T_1$ or $T_b - T_a$. In an MD simulation, $T_b - T_a$ is very straightforward to determine whereas $T_2 - T_1$ is not. Therefore, we have instead developed a theory for σ_K using a definition based on the temperature discontinuity $T_b - T_a$ and interface transmission coefficients $\alpha(\lambda,\vec{k})$. For the $\Sigma 3(111)$ grain boundary, characterized by very weak scattering, the theory is in much better agreement with direct MD simulation.

There is still a high degree of uncertainty that leaves the theoretical predictions only within a factor of about two of the direct MD results. In particular, the theory depends on some approximate treatment of scattering in the bulk. While the new approach given by either Eq. (9) or Eq. (10) is much better for the $\Sigma 3(111)$ grain boundary, the agreement for the $\Sigma 29(001)$ boundary is somewhat worse. To achieve better agreement, we think a more detailed understanding of bulk scattering is needed. For example, we might imagine going beyond the approximations outlined above and use the standard expression for normal and umklapp scattering rates $\tau(\lambda,\vec{k})^{-1} = B\omega(\lambda,\vec{k})^2$. We have in fact tried this but found that our results did not converge uniformly as we improved our sampling of the Brillouin zone due to the $(\frac{1}{\omega})^2$ dependence of the scattering time. It was therefore not possible to obtain an unambiguous result. However, it should still be possible to further improve upon the constant relaxation time and mean-free path approximations to achieve better results. One approach would be to use atomistic techniques outlined in Ref. 14 to compute accurate phonon relaxation times.

These observations help elucidate the practical and conceptual challenge of making comparisons between theoretical models and experiments. For example, many experimental configurations measure $T_2 - T_1$. In this case, the direct MD simulations, which most conveniently compute $T_b - T_a$, may not result in predictions for σ_K that can compare meaningfully to experiment. Instead, one can determine $T_b - T_a$ from direct MD simulation, and then use Eqs. (2) and (3) to estimate $T_2 - T_1$, hence obtaining a value of σ_K that can be directly compared to experiment. By contrast, sometimes one is able to determine an "effective" conductivity κ_{eff}. For example, in a polycrystalline or nanocrystalline material, we can assume that

$$\kappa_{\text{eff}} = \frac{\kappa}{1 + \frac{\kappa}{\sigma_K d}}, \tag{11}$$

where κ is the bulk thermal conductivity and d is the grain size. In this case, it is more appropriate to consider σ_K in terms of the discontinuity $T_b - T_a$. The concept of using the right temperature difference is also discussed in Ref. 15.

Another interesting possibility suggested by this work is that there is a close connection between σ_K and the scattering occurring in the bulk. In particular, when σ_K is defined based on $T_b - T_a$, Eq. (8) suggests that σ_K depends on the details of bulk scattering and not solely on what happens at the inter-

face. This point is established through comparison of the predictions obtained from Eq. (9) to those of Eq. (10), which differ only in how bulk scattering is approximately treated. However, it is interesting to consider what might happen with dopants or point defects that have scattering rates $\tau^{-1} = A\omega^4$, or even the limit of nanoscale grain size. In this case, scattering due to details in the bulk of the material or at neighboring grain boundaries, appear to have an effect on the discontinuity $T_b - T_a$. The connection between bulk and interface scatterings is largely unexplored but may provide a path for greater understanding or control of interfacial properties. For nanoscale systems, our results also suggest the possibility that interfacial scattering events cannot be treated separately.

ACKNOWLEDGMENTS

Sandia is a multiprogram laboratory operated by Sandia Corporation, a Lockheed Martin Co., for the National Nuclear Security Administration, U.S. Department of Energy under Contract No. DE-AC04-94AL85000. This work has been supported by the Sandia Laboratory-Directed Research and Development (LDRD) program.

[1] P. L. Kapitza, J. Phys. (USSR) **4**, 181 (1941).
[2] E. T. Swartz and R. O. Pohl, Rev. Mod. Phys. **61**, 605 (1989).
[3] P. K. Schelling, S. R. Phillpot, and P. Keblinski, Phys. Rev. B **65**, 144306 (2002).
[4] P. K. Schelling, S. R. Phillpot, and P. Keblinski, Appl. Phys. Lett. **80**, 2484 (2002).
[5] P. K. Schelling, S. R. Phillpot, and P. Keblinski, J. Appl. Phys. **95**, 6082 (2004).
[6] C. Kimmer, S. Aubry, A. Skye, and P. K. Schelling, Phys. Rev. B **75**, 144105 (2007).
[7] D. A. Young and H. J. Maris, Phys. Rev. B **40**, 3685 (1989).
[8] S. Pettersson and G. D. Mahan, Phys. Rev. B **42**, 7386 (1990).
[9] J. A. Katerberg, C. L. Reynolds, and A. C. Anderson, Phys. Rev. B **16**, 673 (1977).
[10] F. H. Stillinger and T. A. Weber, Phys. Rev. B **31**, 5262 (1985).
[11] T. Watanabe, B. Ni, P. K. Schelling, P. Keblinski, and S. R. Phillpot, J. Appl. Phys. **102**, 063503 (2007).
[12] W. A. Little, Can. J. Phys. **37**, 334 (1959).
[13] S. Simons, J. Phys. C **7**, 4048 (1974).
[14] A. J. H. McGaughey and M. Kaviany, Phys. Rev. B **69**, 094303 (2004).
[15] A. J. H. McGaughey and J. Li, Proceedings of the IMECE 2006 ASME International Mechanical Engineering Conference and Exhibition, Chicago, 5–10 November 2006 (unpublished).